BCSJ

Activation of C–S Bond by Group 10 Metal Complexes: Reaction of Phosphine Ligand Tethered with Three *tert*-Butylthiophenyl Groups with Group 10 Metal Compounds

Nobuhiro Takeda,* Yusuke Tanaka, Rin Oma, Fumiaki Sakakibara, and Masafumi Unno

Division of Molecular Science, and International Education and Research Center for Silicon Science, Graduate School of Science and Technology, Gunma University, 1-5-1 Tenjin-cho, Kiryu, Gunma 376-8515

E-mail: ntakeda@gunma-u.ac.jp

Received: March 17, 2016; Accepted: May 31, 2016; Web Released: May 24, 2016

Nobuhiro Takeda

Nobuhiro Takeda received his B.S. in 1992 and Ph.D. in 1997 from The University of Tokyo under the supervision of Prof. Renji Okazaki. He worked as a postdoctoral fellow at Chiba University (1997–1998) and Institute for Molecular Science (1998). He became an Assistant Professor at Kyushu University in 1998 and moved to Kyoto University as an Assistant Professor in 2000. In 2006, he joined Gunma University as an Associate Professor. His current research interest is focused on synthesis of new ligands and synthesis, structure, and reactivity of their transition-metal complexes.

Abstract

A new PS_3-type tripodal tetradentate ligand, P(2-*t*-BuSC_6H_4)$_3$ (**1b**), was synthesized by reaction of PCl_3 with 2-*t*-Bu$S(C_6H_4)$Li. Reaction of ligand **1b** with $NiCl_2 \cdot 6H_2O$ resulted in the elimination of *t*-BuCl to afford the corresponding 5-coordinate nickel complex, [NiCl{P(2-SC_6H_4)(2-*t*-BuSC_6H_4)$_2$}] **6**. In addition, ligand **1b** reacted with [$PdCl_2$(PhCN)$_2$] and [$PtCl_2$(cod)] to give 4-coordinate square planar palladium and platinum complexes, [MCl{P(2-SC_6H_4)(2-*t*-BuSC_6H_4)$_2$}] (**7**: M = Pd, **8**: M = Pt), respectively, via the elimination of *t*-BuCl. Further elimination of *t*-BuCl from palladium complex **7** proceeded by heating of **7** in $CDCl_3$ at 100 °C for 4 h to form dipalladium complex, [Pd_2{P(2-SC_6H_4)$_2$(2-*t*-BuSC_6H_4)}$_2$] (**9**). The isopropyl-substituted palladium and platinum complexes, [PdCl{P(2-*i*-PrSC_6H_4)$_3$}]Cl (**3a**) and [$PtCl_2${P(2-*i*-PrSC_6H_4)$_3$}] (**5**), also underwent the elimination of *i*-PrCl by the thermolysis in $CDCl_3$ at 60 °C to afford the corresponding complexes, [MCl{P(2-SC_6H_4)(2-*i*-PrSC_6H_4)$_2$}] (**11**: M = Pd, **12**: M = Pt). The structures of these complexes were determined by NMR spectroscopy, elemental analyses, and X-ray crystallography.

C–S bond activation by transition metals has been attracting much attention from the standpoint of catalytic and stoichiometric transformations using organosulfur compounds[1] and hydrodesulfurization (HDS), which is important in petrochemistry.[2–4] In addition, alkylthio groups such as *tert*-butylthio and benzylthio groups have been used as protective groups for thiols, and the C–S bond of these *S*-alkyl thioethers are cleaved by the reaction with (a) Na/NH_3, (b) protic acid such as FSO_3H–SbF_5 and $HClO_4/CH_3CO_2H$, or (c) transition-metal compounds such as silver(I), mercury(II), and copper(II).[5] However, the cleavage of bonds between sp^3 carbon and sulfur atoms catalyzed by nickel(II)[6,7] and palladium(II)[8,9] complexes is relatively rare, and such cleavage catalyzed by platinum(II)[9,10] is very rare.

In recent years, much attention has been focused on transition-metal complexes with tripodal tetradentate ligands due to not only their unique structure and properties but also the potential for the activation of small molecules such as N_2, O_2, and H_2, the stabilization of reactive intermediates, and catalytic activities.[11–16] Recently, we reported the synthesis of a new tripodal tetradentate ligand, tris(2-isopropylthiophenyl)phosphine (**1a**), and their group 10 metal complexes, that is, 5-coordinate nickel(II) and palladium(II) complexes, **2** and **3a**, **4**, respectively, and square planar platinum(II) complex **5** (Chart 1).[17,18]

In this paper, we report the synthesis of the *tert*-butyl derivative of phosphine ligand **1a**, tris(2-*tert*-butylthiophenyl)phosphine (**1b**), and its reactions with group 10 metal complexes. These reactions resulted in the cleavage of the C(sp^3)–S bond along with the elimination of *tert*-butyl chloride. In addition, we report thermolysis of the isopropyl-substituted palladium and platinum complexes, **3a** and **5**, resulting in the C(sp^3)–S bond cleavage with the elimination of isopropyl chloride.

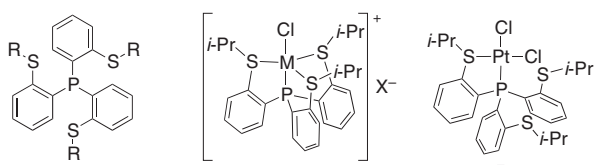

Chart 1. Ligands **1a**, **b**, and group 10 metal complexes with ligand **1a**.

Results and Discussion

Synthesis and Structure of Tris(2-*tert*-butylthiophenyl)-phosphine Ligand (1b). Lithiation of *tert*-butyl phenyl sulfide[19] with butyllithium in the presence of tetramethylethylenediamine (TMEDA) in hexane at 50 °C for 1 h,[20] followed by treatment with PCl_3 at −40 to 25 °C yielded the desired ligand, tris(2-*tert*-butylthiophenyl)phosphine (**1b**), in 43% yield (Scheme 1). Phosphine **1b** is stable in air and its structure was determined by ^1H, ^{13}C, and ^{31}P NMR spectra, elemental analysis, and X-ray crystallographic analysis.

The ORTEP drawing of **1b** showed the pre-organized structure for the 4-coordination to metals with a C_3 symmetry axis, in which the three sulfur atoms are situated on the same side with the lone pair of the phosphorus atom (Figure 1).

Reactions of Ligand 1b with Group 10 Metal Compounds. When ligand **1b** was treated with $NiCl_2 \cdot 6H_2O$ in butanol at 50 °C for 1 d, one *tert*-butyl group on the sulfur atom of **1b** was eliminated to form the corresponding chlorido(thiolato)nickel complex **6** in 89% yield (Scheme 2). Reactions of **1b** with $[PdCl_2(PhCN)_2]$ in $CHCl_3$ at 25 °C for 72 h and with $[PtCl_2(cod)]$ in CH_2Cl_2 at 25 °C for 48 h also resulted in the elimination of *tert*-butyl chloride to afford the corresponding palladium and platinum complexes, **7** and **8**, respectively. The structures of these complexes, **6**, **7**, and **8**, were determined by the ^1H, ^{13}C, and ^{31}P NMR spectra, elemental analyses, and X-ray crystallographic analyses.

The X-ray analyses showed 5-coordinate trigonal-bipyramidal structure of nickel complex **6** (Figure 2) and 4-coordinate square-planar structure of palladium and platinum complexes, **7** and **8** (Figures 3 and 4). In the latter structures, one thioether moiety coordinates to the metal, while another uncoordinates.

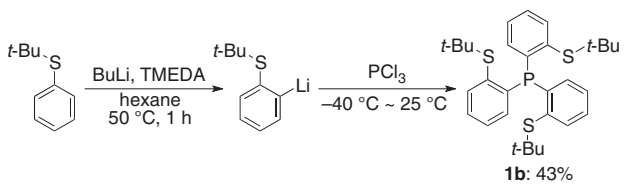

Scheme 1. Synthesis of ligand **1b**.

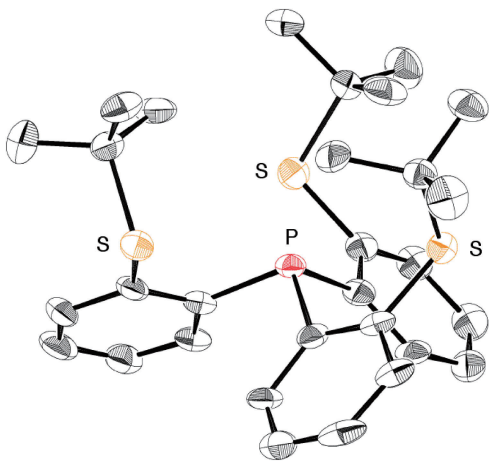

Figure 1. ORTEP drawing of **1b** with thermal ellipsoids (50% probability). All H atoms and solvent molecules have been omitted for clarity.

Table 1 shows selected bond lengths and angles for complexes **6**–**8**. In nickel complex **6**, the Ni1–S1 (thiolato) bond is slightly shorter than the Ni1–S3 (thioether) bond. This tendency is consistent with the reported properties that metal–thiolato bonds are shorter than metal–thioether bonds.[21] The Ni1–S2 bond is longer than the other two Ni–S bonds, the S3–Ni1–S1 bond angle is larger than the other two S–Ni–S bond angles, and the

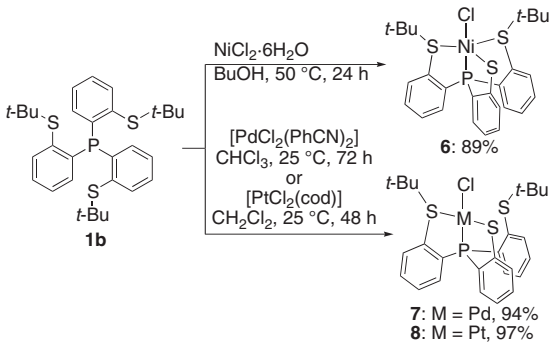

Scheme 2. Reaction of ligand **1b** with group 10 metal complexes.

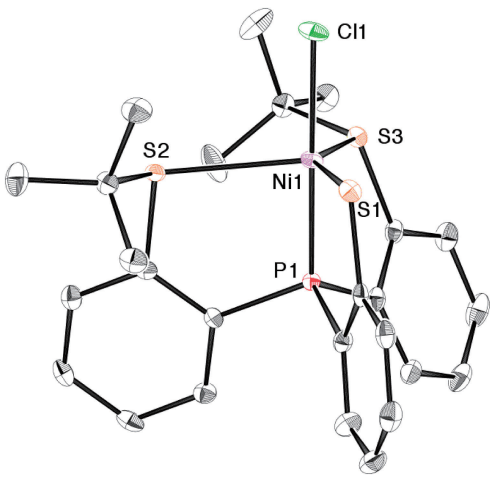

Figure 2. ORTEP drawing of **6** with thermal ellipsoids (50% probability). All H atoms have been omitted for clarity.

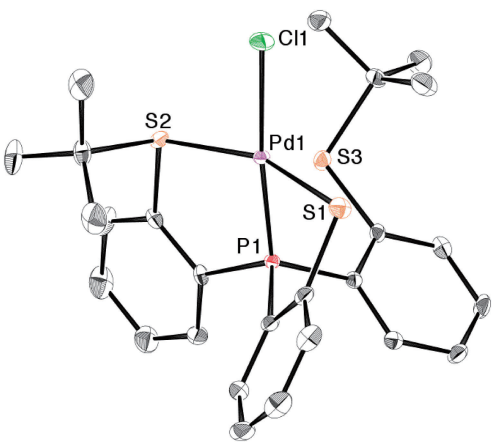

Figure 3. ORTEP drawing of **7** with thermal ellipsoids (50% probability). All H atoms and a solvent molecule have been omitted for clarity.

P1–Ni1–Cl1 bond angle is near 180°. These properties suggest that the 5-coordinate structure of **6** can be explained by the weak coordination of the S2 atom to the distorted square-planar structure constructed by the Ni1, P1, Cl1, S1, and S3 atoms, as in the case of cationic 5-coordinate nickel and palladium complexes, **2**, **3a**, and **4**.[17] Also in the palladium and platinum complexes, **7** and **8**, the M1–S1 (thiolato) bond is slightly shorter than the M1–S2 (thioether) bond. The S1–M1–S2 angles of **7** and **8** deviate from 180°, although the P1–M1–Cl1 and other bond angles around the metal center are close to 180 and 90°, respectively. Therefore, complexes **7** and **8** have distorted square-planar structures. The Pd1–S3 distance (3.4911(7) Å) of **7** is close to the sum of van der Waals radii of Pd (1.63 Å) and S (1.80 Å),[22] suggesting very weak interaction between the Pd1 and S3 atoms. On the other hand, the Pt1–S3 distance (3.862(3) Å) is longer than the sum of van der Waals radii of Pt (1.72 Å) and S (1.80 Å),[22] indicating no interaction between the Pt1 and S3 atoms. The difference in the structure among **6**, **7**, and **8** is consistent with the reported tendency to form five-coordinate complex in the order of $Ni^{II} > Pd^{II} > Pt^{II}$.[23]

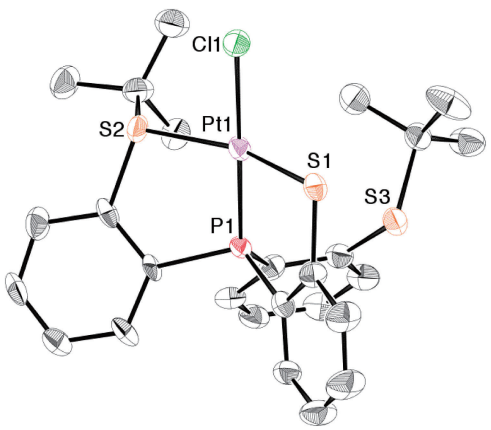

Figure 4. ORTEP drawing of **8** with thermal ellipsoids (50% probability). All H atoms and solvent molecules have been omitted for clarity.

The ^{1}H and ^{13}C NMR spectra of **6**–**8** showed that the two *tert*-butyl groups are equivalent, although those in the crystalline states are nonequivalent. Since these results suggest the rapid interconversion between the two *tert*-butyl groups in solution on the time scale of NMR spectrometry at room temperature, variable temperature NMR experiments were examined. The ^{1}H NMR spectrum of platinum complex **8** at −60 °C indicated splitting of the methyl peak of the *tert*-butyl group into two peaks at 1.18 and 1.28 ppm with the ratio of 1:1, and the $^{31}P\{^{1}H\}$ and $^{195}Pt\{^{1}H\}$ NMR spectra at −60 °C showed one set of peaks, that is, one singlet peak with a pair of satellite peaks on the $^{31}P\{^{1}H\}$ NMR spectrum and one doublet peak on the $^{195}Pt\{^{1}H\}$ NMR spectrum. These spectra at −60 °C are consistent with 4-coordinate structures, **A** and **B**, and 5-coordinate structure **C** shown in Chart 2. Since X-ray structural analysis often indicates the most stable structure, it is considered that the structure in solution at −60 °C is structure **A** observed in X-ray crystallography (Figure 4). However, the possibility of rapid interconversion between structures **A** and **B** by pyramidal inversion on the sulfur atom coordinating to the platinum center cannot be rejected. Platinum complex **8**, in solution at room temperature, is thought to undergo rapid interconversion between the coordinating and non-coordinating sulfur atoms in the 4-coordinate structure. Similar rapid interconversion has been observed in platinum complex **5**.[17] On the other hand, in the ^{1}H NMR spectrum of palladium complex **7** at −60 °C, the broadening of peaks was observed. It is analogized that palladium complex **7** also undergoes similar rapid interconversion between the coordinating and non-coordinating sulfur atoms in the 4-coordinate structure in solution at room temperature. As for nickel complex **6**, rapid interconversion between 4- and 5-

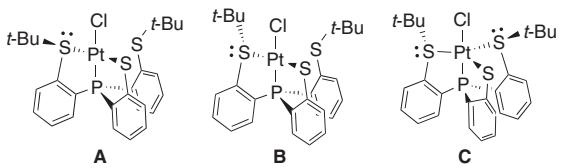

Chart 2. Possible structures of complex **8** in solution.

Table 1. Selected bond lengths (Å) and angles (°)

	6	7	8	11	12
M1–S1	2.2012(6)	2.3251(7)	2.287(3)	2.3089(7)	2.2895(11)
M1–S2	2.6378(6)	2.3548(7)	2.297(3)	2.3816(7)	2.2919(11)
M1–S3	2.2521(6)	3.4911(7)	3.862(3)	3.1214(7)	3.797(1)
M1–Cl1	2.2289(6)	2.3769(7)	2.360(3)	2.3753(6)	2.3740(12)
M1–P1	2.1002(6)	2.1731(7)	2.197(3)	2.1705(6)	2.1888(11)
Cl1–M1–S1	90.03(2)	96.28(3)	91.01(11)	91.76(2)	93.01(4)
Cl1–M1–S2	95.82(2)	95.85(3)	90.98(11)	99.22(2)	90.82(4)
Cl1–Ni1–S3	93.45(2)				
P1–M1–S1	87.94(2)	81.15(3)	88.68(11)	82.18(3)	88.69(4)
P1–M1–S2	84.79(2)	87.98(3)	88.81(11)	87.99(2)	87.69(4)
P1–Ni1–S3	88.19(2)				
P1–M1–Cl1	177.96(3)	174.41(3)	178.58(12)	171.18(2)	178.25(4)
S1–M1–S2	107.27(2)	160.46(3)	158.72(12)	164.51(2)	162.08(4)
S2–Ni1–S3	108.92(2)				
S3–Ni1–S1	143.07(2)				
Sum of bond angles	359.26[a)]	361.26[b)]	359.48[b)]	361.15[b)]	360.21[b)]

a) Sum of bond angles among S1–Ni1–S2, S2–Ni1–S3, and S3–Ni1–S1. b) Sum of bond angles around the metal.

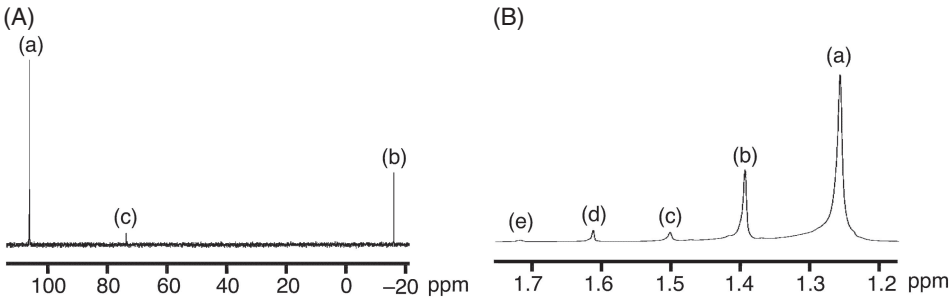

Figure 5. The $^{31}P\{^{1}H\}$ (A) and ^{1}H (B) NMR spectra of the reaction mixture in the reaction of **1b** with $[PdCl_2(PhCN)_2]$ in $CDCl_3$. (a) is a new peak, (b) denotes **1b**, (c) denotes **7**, (d) denotes *t*-BuCl, and (e) denotes isobutene.

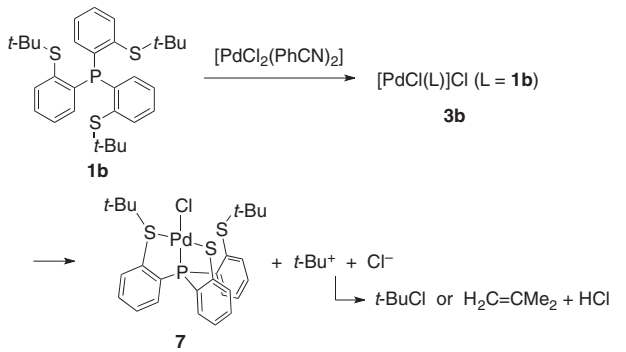

Scheme 3. Plausible mechanism for the formation of **7**.

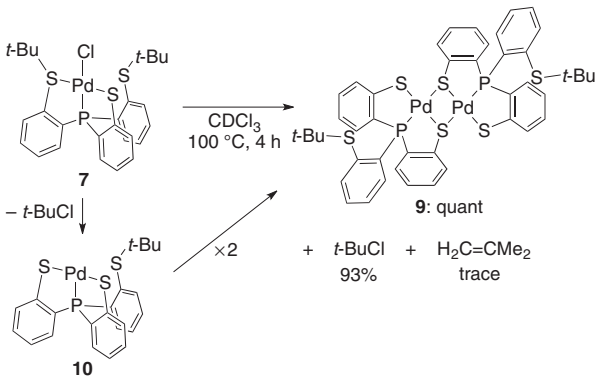

Scheme 4. Thermal reaction of palladium complex **7**.

coordinate structures or rapid pyramidal inversion on the sulfur atoms in the 5-coordinate structure is suggested in solution at room temperature.

In order to investigate the reaction mechanism, the reaction of ligand **1b** with $[PdCl_2(PhCN)_2]$ in $CDCl_3$ in an NMR tube was monitored by ^{1}H and $^{31}P\{^{1}H\}$ NMR spectrometry. After standing of the reaction mixture at room temperature for 10 min, the $^{31}P\{^{1}H\}$ NMR spectrum showed a large peak at 105.9 ppm together with small peaks at 73.7 (for **7**) and −15.7 (for **1b**) ppm. In the ^{1}H NMR spectrum, a large peak at 1.26 ppm was observed along with small peaks at 1.40 (for **1b**), 1.50 (for **7**), 1.61 (for *t*-BuCl), and 1.72 (t, $^{4}J_{HH} = 1.2$ Hz, for isobutene[24]) ppm (Figure 5). Further reaction at room temperature for 3 days resulted in the disappearance of these large peaks at δ_P 105.9 ppm and δ_H 1.26 ppm, which is assigned to [PdCl(L)]Cl (L = **1b**) (**3b**), and almost quantitative formation of **7** (δ_P 73.7 ppm, δ_H 1.51 ppm) was observed together with the formation of *t*-BuCl and isobutene with a molar ratio of **7**:*t*-BuCl:isobutene = 5:4:1.

Thus, it is considered that the reaction of **1b** with $[PdCl_2(PhCN)_2]$ initially affords complex **3b**, and then **3b** undergoes the cleavage of the C(*t*-Bu)–S bond activated by the coordination of the sulfur atoms to the acidic divalent palladium center and the resulting *tert*-butyl cation affords *t*-BuCl or isobutene via addition of chloride anion or elimination of H^+, respectively (Scheme 3). The formation of nickel complex **6** and platinum complex **8** can be explained by a similar mechanism. Also in the C–S bond cleavage catalyzed by Lewis acids such as H^+, Ag^+, Hg^{2+}, Cu^{2+}, etc., similar types of mechanism have been postulated.[5] Cleavage of C(sp^3)–S bond activated by nickel(II)[6,7] and palladium(II)[8,9] complexes is relatively rare, and such cleavage catalyzed by platinum(II)[9] is very rare as described above, therefore, these results are interesting. In addition, this mechanism is consistent with the stability of the isopropyl-substituted group 10 metal complexes **2**–**5**.[17] Since *tert*-butyl cation is more stable than isopropyl cation, the *tert*-butyl derivatives undergo easy elimination of *tert*-butyl cation to afford complexes **6**–**8**.

Thermolysis of Palladium Complex 7. It is expected that group 10 metal complexes **6**–**8** bearing two *tert*-butylthio groups and one chlorido ligand can undergo the further elimination of *tert*-butyl chloride by thermal reaction to afford the corresponding complexes coordinated by one phosphine part and two thiolato parts. We examined thermal reaction of palladium complex **7**.

When a $CDCl_3$ solution of **7** was heated at 100 °C for 4 h in a sealed tube, dipalladium complex **9** and *t*-BuCl, which is confirmed by ^{1}H and ^{13}C NMR spectra [δ_H 1.62 ppm; δ_C 34.5 (q), 67.1 (s) ppm], were quantitatively formed together with a trace amount of isobutene (Scheme 4). The structure of complex **9** was determined by ^{1}H, ^{13}C, and ^{31}P NMR spectra, UV–vis spectrum, elemental analysis and X-ray crystallographic analysis.

The X-ray analysis showed that the complex **9** has nearly C_2 symmetry and the two palladium atoms are bridged by two thiolato ligands to give the Pd_2S_2 four-membered ring (Figure 6). Each palladium atom is further coordinated by one phosphine and one thiolato ligands. The sums of bond angles around the two palladium atoms are near 360° (358.7° for Pd1 and 358.9° for Pd2), therefore, the two palladium atoms have distorted square-planar structures. The angle between the two planes (the plane including Pd1, P1, S1, S2, and S4 and the plane including Pd2, P2, S1, S4, and S5) is 65.8° and the Pd_2S_2 four-membered ring has a bent structure. The two C_6H_4S(*t*-Bu) groups on the phosphorus atoms are situated in the open side of

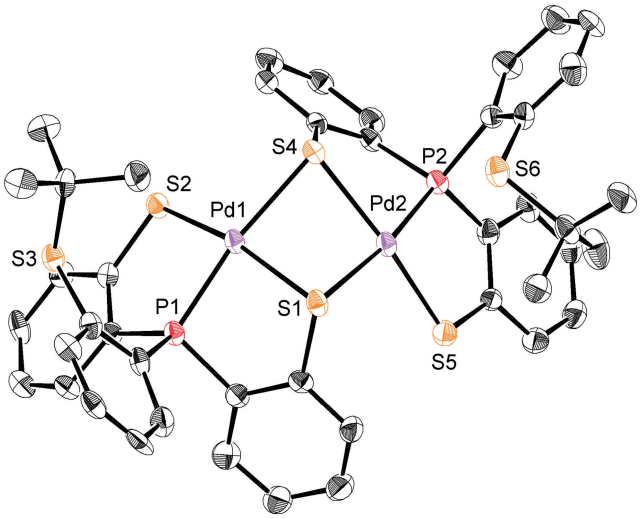

Figure 6. ORTEP drawing of **9** with thermal ellipsoids (50% probability). All H atoms and a solvent molecule have been omitted for clarity. Selected bond lengths (Å) and angles (deg): Pd1–Pd2, 3.0848(8); Pd1–P1, 2.218(2); Pd1–S1, 2.369(2); Pd1–S2, 2.296(2); Pd1–S4, 2.420(2); Pd2–P2, 2.195(2); Pd2–S4, 2.368(2); Pd2–S5, 2.313(2); Pd2–S1, 2.414(2); P1–Pd1–S2, 87.60(7); P1–Pd1–S1, 84.36(7); S2–Pd1–S4, 98.04(7); S1–Pd1–S4, 88.69(7); P2–Pd2–S5, 86.90(8); S5–Pd2–S1, 99.27(8); S4–Pd2–S1, 88.85(7); P2–Pd2–S4, 83.84(8).

the Pd_2S_2 ring with *cis* configuration in order to avoid steric congestion. In the reflection of *trans* influence, the Pd–(μ^2-S) bonds (Pd1–S4, 2.420(2) and Pd2–S1, 2.414(2) Å) situated in the *trans* position of the phosphine ligands are longer than the other Pd–S bonds. The bridged Pd–(μ^2-S) bonds (Pd1–S1, 2.369(2) and Pd2–S4, 2.368(2) Å) are slightly longer than the Pd–(μ^1-S) bonds (Pd1–S2, 2.296(2) and Pd2–S5, 2.313(2) Å). The ^{1}H and ^{13}C NMR spectra indicated that the two *tert*-butyl groups are equivalent, and the ^{31}P NMR spectrum showed the only one peak. In addition, no change was observed in the ^{1}H and ^{31}P NMR spectra of **9** at −60 °C. These results strongly suggest that the structure in solution is similar to that in the crystalline state. This nonfluxional structure of **9** may be explained by the stronger bonds between palladium and thiolato ligands compared with coordination of thioether ligands to the palladium center.

The formation mechanism of complex **9** can be explained by the elimination of *tert*-butyl chloride from chloridopalladium complex **7** and the subsequent dimerization of the resulting unsaturated three-coordinate palladium(II) complex **10** (Scheme 4). Instability of intermediate **10** may rationalize the elimination of *tert*-butyl chloride from **7** at higher temperature compared with the temperature in the formation of **7** along with *tert*-butyl chloride.

Thermolysis of Group 10 Metal Complexes with Isopropyl-Substituted Ligand, 3a and 5. It is considered that complexes **6**–**8** are formed via the elimination of *tert*-butyl cation from the group 10 metal complexes bearing ligand **1b**, [MCl(L)]Cl (M = Ni, Pd, Pt; L = **1b**) at 25 or 50 °C. This consideration suggests the possibility of the elimination of isopropyl chloride from the isopropyl derivatives **2**–**5**.

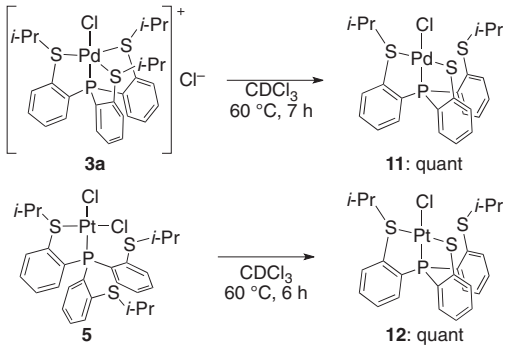

Scheme 5. Thermal reaction of isopropyl derivatives **3a** and **5**.

When thermal reaction of palladium complex **3a** in $CDCl_3$ was monitored by ^{1}H NMR spectroscopy, heating of **3a** at 60 °C for 7 h resulted in quantitative formation of complex **11** along with the formation of isopropyl chloride [δ_H 1.52 (d, $^3J_{HH}$ = 7 Hz, 6H), 4.20 (d, $^3J_{HH}$ = 7 Hz, 1H) ppm; δ_C 27.2 (q), 53.9 (d) ppm] (Scheme 5). Thermal reaction of platinum complex **5** in $CDCl_3$ at 60 °C for 6 h monitored by ^{1}H NMR spectroscopy also afforded platinum complex **12** together with isopropyl chloride. These reactions support the above-mentioned mechanism for the formation of complexes **6**–**8** via [MCl(L)]Cl (M = Ni, Pd, Pt; L = **1b**). The easier elimination of *tert*-butyl cation from **6**–**8** than that of isopropyl cation from **3a** and **5** is probably due to the stability of *tert*-butyl cation compared with isopropyl cation as described in the former section. These cleavage reactions of the S–C (*i*-Pr) bond are interesting, because S–C (*i*-Pr) bond cleavage using transition-metal compounds is very rare despite the existence of the cleavage reactions using alkaline metals,[25] tin hydrides,[26,27] or Lewis acids such as $AlCl_3$ and $TiCl_4$.[28]

The structures of complexes **11** and **12** were determined by ^{1}H, ^{13}C, and ^{31}P NMR spectra, elemental analysis, and X-ray crystallography. The NMR spectra and X-ray crystallography indicated the similar tendency to those of *tert*-butyl derivatives, **7** and **8** (Table 1 and Figures 7 and 8).

On the other hand, thermolysis of chloridonickel and chloridopalladium tetrafluoroborates, **2** and **4**, at 60 °C resulted in no reaction. These results may be explained by the instability of the expected products, cationic complexes having a vacant coordination site, [M{P(2-SC_6H_4)(2-*t*-BuSC_6H_4)$_2$}]BF_4 (M = Ni, Pd), as well as the case of the elimination of *tert*-butyl group from **7**.

Conclusion

In summary, we synthesized a new PS_3-type tripodal tetradentate ligand **1b** bearing *tert*-butylthio groups. Reaction of **1b** with group 10 metal complexes resulted in the elimination of *tert*-butyl chloride to afford the corresponding complexes, **6**–**8**. In these reactions, it is considered that the corresponding group 10 metal complexes, [MCl(L)]Cl (M = Ni, Pd, Pt; L = **1b**), are initially formed and the C–S bond activated by the coordination of the sulfur atoms to the metal center is subsequently cleaved along with the formation of *tert*-butyl cation. Further elimination of *tert*-butyl chloride from **7** afforded dipalladium complex **9**. In addition, isopropyl derivatives, **11** and **12**, were

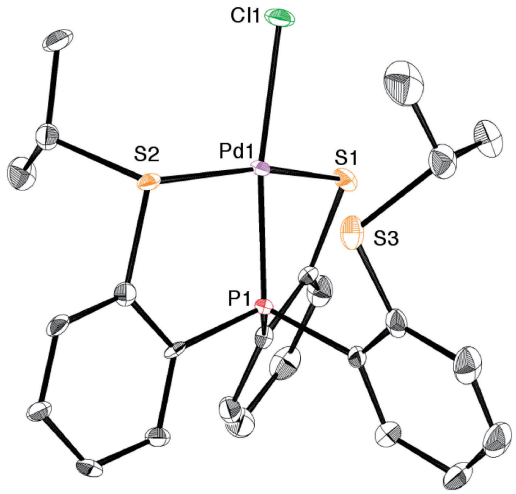

Figure 7. ORTEP drawing of **11** with thermal ellipsoids (50% probability). All H atoms have been omitted for clarity.

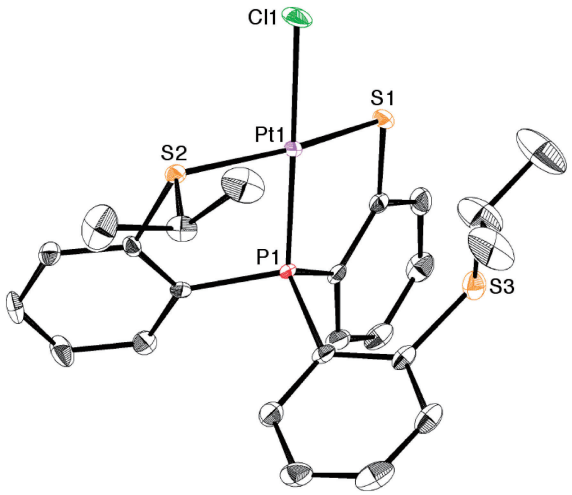

Figure 8. ORTEP drawing of **12** with thermal ellipsoids (50% probability). All H atoms and minor parts of the disordered isopropyl group have been omitted for clarity.

also formed by thermal reactions of **3a** and **5**, respectively. The easier elimination of *tert*-butyl chloride than that of isopropyl chloride is probably due to the stability of *tert*-butyl cation compared with isopropyl cation. The C(sp^3)–S bond cleavage activated by group 10 metal is rare and, especially, the cleavage activated by platinum(II) and the cleavage of the isopropyl–sulfur bond activated by transition metals are very rare. These C(sp^3)–S bond cleavage reactions are very interesting.

It is expected that these results obtained in this paper can contribute to the chemistry of organosulfur compounds and group 10 metal complexes with thioether ligands.

Experimental Section

General Procedures. All reactions were carried out under an argon atmosphere unless otherwise noted. Tetrahydrofuran was purified by distillation from sodium diphenylketyl before use. Other solvents used in reactions were purified by the reported methods.[29] Wet column chromatography (WCC) was performed with Merck Silica Gel 60 (70–230 mesh ASTM). The ^{1}H NMR (600, 500, or 400 MHz), ^{13}C NMR (150 or 126 MHz), ^{31}P NMR (243 or 202 MHz), and ^{195}Pt NMR (129 MHz) spectra were measured in $CDCl_3$ with a JEOL JNM-ECA600, JNM-λ500, or JNM-ECS400 spectrometer using $SiMe_4$ (0 ppm) as internal standards for ^{1}H NMR spectroscopy, $CDCl_3$ (77.0 ppm) as those for ^{13}C NMR spectroscopy, H_3PO_4 (85%) in D_2O (0 ppm) as an external standard for ^{31}P NMR spectroscopy, and Na_2PtCl_6 in D_2O (0 ppm) as an external standard for ^{195}Pt NMR spectroscopy. The UV–vis spectra were recorded on a JASCO V-550 UV–vis spectrometer. All melting points were determined on a Yanaco micro melting point apparatus MP-J3 and are uncorrected. Elemental analyses were performed by the Center for Material Research by Instrumental Analysis (CIA), Gunma University.

Preparation of Tris(2-*tert*-butylthiophenyl)phosphine (1b). To a mixture of *tert*-butyl phenyl sulfide[19] (3.00 g, 18.0 mmol), TMEDA (5.40 mL, 36.0 mmol), and hexane (15 mL) was added a hexane solution of butyllithium (1.65 M, 13.1 mL, 21.6 mmol) at 25 °C. After heating at 60 °C for 1 h, PCl_3 (0.58 ml, 6.60 mmol) was added to the mixture at −40 °C. The reaction mixture was stirred at this temperature for 3 h, then gradually warmed to 25 °C over 12 h. After addition of a saturated aqueous solution of NH_4Cl, the mixture was extracted with hexane. The organic layer was dried over anhydrous $MgSO_4$, and the solvents were removed under reduced pressure. The residue was separated by WCC (SiO_2, hexane:chloroform = 1:1) to afford pure tris(2-*tert*-butylthiophenyl)phosphine (**1b**) (1.35 g, 2.56 mmol, 43%). **1b**: colorless crystals, mp. 204.0–206.0 °C; ^{1}H NMR (500 MHz, $CDCl_3$): δ 1.41 (s, 27H), 6.47 (dd, $^3J_{HH}$ = 7.5 Hz, $^4J_{HH}$ = 1.2 Hz, 3H), 7.15 (ddd, $^3J_{HH}$ = 7.5, 7.5 Hz, $^4J_{HH}$ = 1.2 Hz, 3H), 7.27 (ddd, $^3J_{HH}$ = 7.5, 7.5 Hz, $^4J_{HH}$ = 1.2 Hz, 3H), 7.62 (ddd, $^3J_{HH}$ = 7.5 Hz, $^4J_{HH}$ = 1.5Hz, $^3J_{HP}$ = 4.2 Hz, 3H); ^{13}C{^{1}H} NMR (126 MHz, $CDCl_3$): δ 31.2 (CH_3), 48.4 (C), 127.9 (CH), 130.0 (CH), 133.9 (CH), 137.3 (d, $^1J_{CP}$ = 31 Hz), 138.3 (CH), 147.3 (d, $^2J_{CP}$ = 14 Hz); ^{31}P{^{1}H} NMR (202 MHz, $CDCl_3$): δ −16.6 (s). Anal. Calcd for $C_{30}H_{39}PS_3 \cdot 0.5H_2O$: C, 67.25; H, 7.52%. Found: C, 67.27; H, 7.36%.

Reaction of 1b with $NiCl_2 \cdot 6H_2O$. A mixture of **1b** (100 mg, 0.190 mmol), $NiCl_2 \cdot 6H_2O$ (50 mg, 0.210 mmol), and butanol (2.0 mL) was heated at 50 °C for 24 h. The reaction mixture was allowed to stand at 25 °C to give [NiCl{P(2-SC_6H_4)-(2-*t*-$BuSC_6H_4$)$_2$}] (**6**) (95 mg, 0.168 mmol, 89%) as gray precipitates. **6**: gray crystals, mp 264 °C (decomp); ^{1}H NMR (500 MHz, $CDCl_3$): δ 1.50 (s, 18H), 6.98 (br s, 1H), 7.09–7.69 (m, 9H), 7.76 (br s, 2H). ^{13}C{^{1}H} NMR (126 MHz, $CDCl_3$): δ 30.7 (CH_3), 55.5 (C), 121.8 (d, J_{CP} = 6 Hz, CH), 127.7 (CH), 128.6 (d, $^1J_{CP}$ = 45 Hz), 129.5 (CH), 131.8 (d, J_{CP} = 9 Hz, CH), 132.3 (CH), 133.7 (CH), 135.3 (d, J_{CP} = 9 Hz, CH), 138.1 (CH), 138.5 (d, $^1J_{CP}$ = 60 Hz), 139.2 (d, $^2J_{CP}$ = 19 Hz), 159.0 (d, $^2J_{CP}$ = 28 Hz). ^{31}P{^{1}H} NMR (202 MHz, $CDCl_3$): δ 69.1 (s). UV–vis (chloroform) λ_{max} 272 (ε 10000), 326 (ε 5100), 508 (ε 940), 649 (ε 330) nm. Anal. Calcd for $C_{26}H_{30}ClNiPS_3 \cdot 0.5H_2O$: C, 54.51, H, 5.45%. Found: C, 54.63; H, 5.35%.

Reaction of 1b with [$PdCl_2$(PhCN)$_2$]. A mixture of **1b** (140 mg, 0.266 mmol), [$PdCl_2$(PhCN)$_2$] (100 mg, 0.261 mmol), and chloroform (4.0 mL) was stirred at 25 °C for 72 h. After filtration of the reaction mixture, the filtrate was concentrated.

The residue was reprecipitated by the addition of hexane to a dichloromethane solution of the mixture to afford [PdCl{P(2-SC_6H_4)(2-*t*-BuSC_6H_4)$_2$}] (**7**) (150 mg, 0.245 mmol, 94%). **7**: red crystals, mp 151 °C (decomp); ^{1}H NMR (500 MHz, $CDCl_3$): δ 1.51 (s, 18H), 7.02 (ddd, $^3J_{HH} = 8$, 8 Hz, $J_{HP} = 3$ Hz, 1H), 7.23–7.31 (m, 4H), 7.39–7.44 (m, 3H), 7.54 (dd, $^3J_{HH} = 8$, 8 Hz, 2H), 7.70 (dd, $^3J_{HH} = 8$ Hz, $J_{HP} = 4$ Hz, 2H). ^{13}C{^{1}H} NMR (126 MHz, $CDCl_3$): δ 31.4 (CH_3), 55.0 (C), 122.4 (d, $J_{CP} = 9$ Hz, CH), 128.4 (d, $^1J_{CP} = 65$ Hz), 129.3 (d, $J_{CP} = 20$ Hz, CH), 129.4 (d, $J_{CP} = 3$ Hz, CH), 130.2 (CH), 132.1 (CH), 132.9 (CH), 133.1 (d, $J_{CP} = 5$ Hz, CH), 136.3 (d, $J_{CP} = 11$ Hz, CH), 138.5 (d, $^1J_{CP} = 63$ Hz), 139.0 (d, $^2J_{CP} = 17$ Hz), 159.1 (d, $^2J_{CP} = 25$ Hz). ^{31}P{^{1}H} NMR (202 MHz, $CDCl_3$): δ 72.8 (s). UV–vis (chloroform) λ_{max} 336.5 (ε 1800), 384 (ε 570), 451 (ε 110) nm. Anal. Calcd. for $C_{26}H_{30}ClPPdS_3 \cdot CHCl_3$: C, 44.37; H, 4.27%. Found: C, 44.27; H, 4.14%.

Reaction of 1b with [PtCl$_2$(cod)]. A mixture of **1b** (140 mg, 0.266 mmol), [$PtCl_2$(cod)] (100 mg, 0.267 mmol), and dichloromethane (2.0 mL) was stirred at 25 °C for 48 h. After filtration of the reaction mixture, the filtrate was concentrated. The residue was reprecipitated by the addition of hexane to a chloroform solution of the mixture to afford [PtCl{P(2-SC_6H_4)-(2-*t*-BuSC_6H_4)$_2$}] (**8**) (180 mg, 0.257 mmol, 97%). **8**: orange crystals, mp 166 °C (decomp); ^{1}H NMR (500 MHz, $CDCl_3$): δ 1.31 (s, 18H), 6.90 (ddd, $^3J_{HH} = 7$, 7 Hz, $J_{HP} = 3$ Hz, 1H), 7.20 (dd, $^3J_{HH} = 7$, 7 Hz, 1H), 7.25–7.54 (m, 7H), 7.55 (dd, $^3J_{HH} = 7$ Hz, $J_{HP} = 3$ Hz, 1H), 7.67 (dd, $^3J_{HH} = 8$ Hz, $J_{HP} = 4$ Hz, 2H). ^{13}C{^{1}H} NMR (126 MHz, $CDCl_3$): δ 31.1 (CH_3), 54.2 (C), 122.2 (d, $J_{CP} = 9$ Hz, CH), 127.3 (d, $^1J_{CP} = 76$ Hz), 129.0 (d, $J_{CP} = 4$ Hz, CH), 129.3 (d, $J_{CP} = 17$ Hz, CH), 130.3 (d, $^1J_{CP} = 67$ Hz), 131.9 (CH), 132.17 (d, $J_{CP} = 4$ Hz, CH), 132.22 (d, $J_{CP} = 4$ Hz, CH), 133.5 (d, $J_{CP} = 5$ Hz, CH), 136.4 (d, $J_{CP} = 9$ Hz, CH), 141.4 (d, $J_{CP} = 16$ Hz), 160.6 (d, $J_{CP} = 26$ Hz). ^{31}P{^{1}H} NMR (202 MHz, $CDCl_3$): δ 47.9 (s, $^1J_{PPt} = 3679$ Hz). ^{195}Pt{^{1}H} NMR (129 MHz, $CDCl_3$): δ −4418 (s, $^1J_{PPt} = 3659$ Hz). UV–vis (chloroform) λ_{max} 291.5 (ε 13500), 343.5 (ε 3300), 394.5 (ε 910) nm. Anal. Calcd. for $C_{26}H_{30}ClPPtS_3$: C, 44.60; H, 4.32%. Found: C, 44.50; H, 4.79%.

Thermolysis of 7. In a 5 ϕ NMR tube was placed a $CDCl_3$ solution (0.6 mL) of **7** (30 mg, 0.049 mmol). After three freeze-pump-thaw cycles, the tube was frozen, evacuated, and sealed. The solution was heated at 100 °C for 4 h, during which time the reaction was followed by ^{1}H NMR spectroscopy. The sealed tube was opened, and the reaction mixture was concentrated. The residue was reprecipitated by the addition of hexane to a chloroform solution of the mixture to afford [Pd{P(2-SC_6H_4)$_2$-(2-*t*-BuSC_6H_4)}]$_2$ (**9**) in a quantitative yield.

In order to obtain the yield of *t*-BuCl: In a pressure-resistant NMR tube was placed a $CDCl_3$ solution (0.6 mL) of **7** (29.3 mg, 0.048 mmol) and mesitylene (10 µL, 0.072 mmol as a standard). The solution was gradually warmed to 100 °C and heated at 100 °C for 4 h. The ^{1}H NMR spectrum of the reaction mixture indicated the formation of **9**, *t*-BuCl (integral ratio of mesitylene:*t*-BuCl = 1.0:0.62, 0.045 mmol, 93%) and a trace amount of isobutene. **9**: red crystals, mp 238 °C (decomp); ^{1}H NMR (500 MHz, $CDCl_3$): δ 1.47 (s, 18H), 6.85–6.97 (m, 4H), 6.99 (dd, $^3J_{HH} = 8$, 8 Hz, 2H), 7.13 (dd, $^3J_{HH} = 8$, 8 Hz, 2H), 7.17 (dd, $^3J_{HH} = 8$, 8 Hz, 2H), 7.26–7.23 (m, 2H), 7.36 (d, $^3J_{HH} = 8$ Hz, 2H), 7.41 (dd, $^3J_{HH} = 8$, 8 Hz, 2H), 7.47 (dd, $^3J_{HH} = 8$, 8 Hz, 2H), 7.53 (dd, $^3J_{HH} = 8$, 8 Hz, 2H), 7.58 (d, $^3J_{HH} = 8$ Hz, 2H), 7.63 (dd, $^3J_{HH} = 8$, 8 Hz, 2H). ^{31}P{^{1}H} NMR (202 MHz, $CDCl_3$): δ 63.2 (s). UV–vis (chloroform) λ_{max} 294 (ε 35000), 323 (ε 21000), 366 (ε 16000), 541 (ε 640) nm. Anal. Calcd. for $C_{44}H_{42}P_2Pd_2S_6 \cdot CHCl_3$: C, 46.70; H, 3.74%. Found: C, 46.37; H, 3.91%.

Thermolysis of [PdCl{P(2-*i*-PrSC$_6$H$_4$)$_3$}]Cl (3a). In a 5 ϕ NMR tube was placed a $CDCl_3$ solution (0.5 mL) of **3a** (30 mg, 0.045 mmol). After three freeze-pump-thaw cycles, the tube was frozen, evacuated, and sealed. The solution was heated at 60 °C for 7 h, during which time the reaction was followed by ^{1}H NMR spectroscopy. The sealed tube was opened, and the reaction mixture was concentrated. The residue was reprecipitated by the addition of hexane to a chloroform solution of the mixture to afford [Pd{P(2-SC_6H_4)(2-*i*-PrSC_6H_4)$_2$}] (**11**) in a quantitative yield. **11**: red crystals, mp 227 °C (decomp); ^{1}H NMR (400 MHz, $CDCl_3$): δ 1.33 (d, $^3J_{HH} = 7$ Hz, 6H), 1.48 (d, $^3J_{HH} = 7$ Hz, 6H), 3.77 (sep, $^3J_{HH} = 7$ Hz, 2H), 7.01 (ddd, $^3J_{HH} = 7$, 7 Hz, $J_{HP} = 3$ Hz, 1H), 7.24–7.42 (m, 7H), 7.55 (ddd, $^3J_{HH} = 8$ Hz, $^4J_{HH} = 2$ Hz, $J_{HP} = 2$ Hz, 2H), 7.65 (dd, $^3J_{HH} = 8$ Hz, $J_{HP} = 4$ Hz, 2H). ^{13}C{^{1}H} NMR (126 MHz, $CDCl_3$): δ 22.3 (CH_3), 23.5 (CH_3), 45.7 (CH), 122.4 (d, $J_{CP} = 9$ Hz, CH), 128.5 (d, $^1J_{CP} = 66$ Hz), 129.1 (d, $J_{CP} = 8$ Hz, CH), 129.5 (d, $J_{CP} = 20$ Hz, CH), 130.3 (CH), 132.7 (d, $J_{CP} = 2$ Hz, CH), 132.9 (d, $J_{CP} = 5$ Hz, CH), 133.0 (CH), 134.7 (d, $J_{CP} = 10$ Hz, CH), 136.5 (d, $^1J_{CP} = 61$ Hz), 139.8 (d, $^2J_{CP} = 18$ Hz), 159.0 (d, $^2J_{CP} = 25$ Hz). ^{31}P{^{1}H} NMR (202 MHz, $CDCl_3$): δ 72.0 (s). Anal. Calcd. for $C_{24}H_{26}ClPPdS_3$: C, 49.40; H, 4.49%. Found: C, 49.24; H, 4.30%.

Thermolysis of [PtCl$_2${P(2-*i*-PrSC$_6$H$_4$)$_3$}] (5). In a 5 ϕ NMR tube was placed a solution of **5** (13 mg, 0.017 mmol) in $CDCl_3$ (0.5 mL). The solution was heated at 60 °C for 6 h, during which time the reaction was followed by ^{1}H NMR spectroscopy. The ^{1}H NMR spectrum of the reaction mixture showed quantitative formation of [Pt{P(2-SC_6H_4)(2-*i*-PrSC_6H_4)$_2$}] (**12**).

For isolation of **12**, see: A solution of **5** (100 mg, 0.133 mmol) in chloroform (4 mL) was heated at 60 °C for 48 h. After filtration of the reaction mixture, the filtrate was concentrated. The residue was reprecipitated by the addition of hexane to a chloroform solution of the mixture to give [Pt{P(2-SC_6H_4)(2-*i*-PrSC_6H_4)$_2$}] (**12**) (73 mg, 0.109 mmol, 82%). **12**: orange crystals, mp 213 °C (decomp); ^{1}H NMR (600 MHz, $CDCl_3$, 60 °C): δ 1.22 (br d, $^3J_{HH} = 6.6$ Hz, 6H), 1.26 (br d, $^3J_{HH} = 6.6$ Hz, 6H), 3.53 (br s, 2H), 6.90–6.95 (m, 1H), 7.14–7.19 (m, 1H), 7.31–7.51 (m, 8H), 7.56–7.60 (m, 2H). ^{13}C{^{1}H} NMR (150 MHz, $CDCl_3$, 60 °C): δ 22.1 (s, CH_3), 22.9 (s, CH_3), 44.8 (br s, CH), 122.4 (d, $J_{CP} = 8.6$ Hz, CH), 127.5 (d, $^1J_{CP} = 74.6$ Hz), 129.1 (br s, CH), 129.7 (d, $J_{CP} = 11.0$ Hz, CH), 131.3 (s, CH), 132.6 (s, CH), 132.7 (s, CH), 133.0 (br s, CH), 134.7 (br d, $J_{CP} = 6.0$ Hz, CH), 135.5 (d, $^1J_{CP} = 67.5$ Hz), 141.9 (br d, $^2J_{CP} = 15.9$ Hz), 160.6 (br d, $^2J_{CP} = 21.5$ Hz). ^{31}P{^{1}H} NMR (243 MHz, $CDCl_3$, 60 °C): δ 50.0 (s, $^1J_{PPt} = 3566$ Hz). ^{31}P{^{1}H} NMR (243 MHz, $CDCl_3$, 20 °C): δ 49.9 (s, $^1J_{PPt} = 3583$ Hz). Anal. Calcd. for $C_{24}H_{26}ClPPtS_3$: C, 42.88; H, 3.90%. Found: C, 42.58; H, 4.18%.

X-Ray Crystallography of 1b·H$_2$O, 6, 7·CH$_2$Cl$_2$, 8·0.5CHCl$_3$, 9·CHCl$_3$, 11, and 12. Single crystals of **1b**·H_2O, **6**, **7**·CH_2Cl_2, **8**·0.5$CHCl_3$, **9**·$CHCl_3$, **11**, and **12** suitable for X-ray structural analysis were obtained by slow recrys-

Table 2. Crystal data and refinement details for **1b**·H_2O, **6**, and **7**·CH_2Cl_2

	1b·0.5H_2O	**6**	**7**·CH_2Cl_2
Empirical formula	$C_{30}H_{39}PS_3$·0.5H_2O	[$C_{26}H_{30}$-ClNiPS_3]	[$C_{26}H_{30}$-ClPPdS_3]·CH_2Cl_2
Formula weight	535.81	563.81	696.43
Temperature/K	123(2)	123(2)	123(2)
Crystal system	trigonal	monoclinic	orthorhombic
Space group	*P*–3 (No. 147)	$P2_1/c$ (No. 14)	$P2_12_12_1$ (No. 19)
a/Å	14.8175(17)	15.3031(10)	9.9862(5)
b/Å	14.8175(17)	10.8984(7)	16.2536(8)
c/Å	8.3455(11)	15.5377(10)	18.7218(9)
α/deg	90	90	90
β/deg	90	100.0947(7)	90
γ/deg	120	90	90
V/Å^3	1586.8(3)	2551.3(3)	3038.8(3)
Z	2	4	4
D_{calc}/Mg m^{-3}	1.136	1.468	1.522
Absorp coeff/mm^{-1}	0.303	1.187	1.149
Crystal size/mm	0.50 × 0.10 × 0.10	0.30 × 0.30 × 0.10	0.30 × 0.15 × 0.15
θ range	2.75 to 28.27°	2.66 to 25.50°	2.63 to 25.50°
No. of reflns measd	4739	17084	20842
No. of indep reflns	2427	4736	5509
R_{int}	0.0413	0.0202	0.0216
Completeness	92.4%	99.6%	97.6%
Data/Restraints/Parameters	2427/0/110	4736/0/289	5509/4/326
Goodness–of–fit on F^2	1.003	1.266	1.274
Final *R* indices [$I > 2\sigma(I)$][a)]	$R_1 = 0.0698$ $wR_2 = 0.1540$	$R_1 = 0.0315$ $wR_2 = 0.0738$	$R_1 = 0.0192$ $wR_2 = 0.1393$
	$wR_2 = 0.1960$	$wR_2 = 0.0629$	$wR_2 = 0.0503$
R indices (all data)[a)]	$R_1 = 0.1328$ $wR_2 = 0.1757$	$R_1 = 0.0317$ $wR_2 = 0.0754$	$R_1 = 0.0192$ $wR_2 = 0.1414$
	$wR_2 = 0.2261$	$wR_2 = 0.0630$	$wR_2 = 0.0503$
Absolute structure parameter			−0.003(18)
Largest diff. peak and hole/e Å^{-3}	0.642 and −0.498	0.300 and −0.261	0.422 and −0.404

a) $R_1 = \Sigma||F_o| - |F_c||/\Sigma|F_o|$, $wR_2 = [(\Sigma w(F_o^2 - F_c^2)^2/\Sigma w(F_o^2)^2]^{1/2}$.

Table 3. Crystal data and refinement details for **8**·0.5$CHCl_3$ and **9**

	8·0.5$CHCl_3$	**9**·$CHCl_3$
Empirical formula	[$C_{26}H_{30}ClPPtS_3$]·0.5$CHCl_3$	[$C_{44}H_{42}P_2Pd_2S_6$]·$CHCl_3$
Formula weight	759.87	1157.24
Temperature/K	123(2)	123(2)
Crystal system	monoclinic	monoclinic
Space group	$P2_1/n$ (No. 14)	$P2_1/c$ (No. 14)
a/Å	10.2504(13)	16.7717(11)
b/Å	18.715(2)	14.4580(9)
c/Å	15.3198(18)	18.7029(13)
α/deg	90	90
β/deg	96.6494(14)	97.2771(9)
γ/deg	90	90
V/Å^3	2919.1(6)	4498.6(5)
Z	4	4
D_{calc}/Mg m^{-3}	1.729	1.709
Absorp coeff/mm^{-1}	5.320	1.361
Crystal size/mm	0.30 × 0.20 × 0.05	0.20 × 0.20 × 0.20
θ range	2.52 to 27.00°	2.76 to 25.50°
No. of reflns measd	22516	30213
No. of indep reflns	6359	7889
R_{int}	0.0472	0.0388
Completeness	99.9%	93.9%
Data/Restraints/Parameters	6359/0/307	7889/0/524
Goodness–of–fit on F^2	1.225	1.264
Final *R* indices [$I > 2\sigma(I)$][a)]	$R_1 = 0.0919$ $wR_2 = 0.1540$	$R_1 = 0.0822$ $wR_2 = 0.0738$
	$wR_2 = 0.1949$	$wR_2 = 0.1761$
R indices (all data)[a)]	$R_1 = 0.0933$ $wR_2 = 0.1757$	$R_1 = 0.0825$ $wR_2 = 0.0754$
	$wR_2 = 0.1957$	$wR_2 = 0.1763$
Extinction coefficient	0.0036(3)	0.0021(3)
Largest diff. peak and hole/e Å^{-3}	2.556 and −2.271	1.519 and −1.132

a) $R_1 = \Sigma||F_o| - |F_c||/\Sigma|F_o|$, $wR_2 = [(\Sigma w(F_o^2 - F_c^2)^2/\Sigma w(F_o^2)^2]^{1/2}$.

tallization from hexane/$CHCl_3$. The crystals were mounted on glass fibers. The intensity data were collected on a Rigaku R-AXIS IV^{++} diffractometer with graphite monochromated Mo Kα radiation ($\lambda = 0.71070$ Å). The structures were solved by direct methods (SHELXS-97[30] or SIR-97[31]), and refined by full-matrix least-squares procedures on F^2 for all reflections (SHELXL-97[30]). All the non-hydrogen atoms were refined anisotropically. All hydrogens were placed using AFIX instructions. The crystal data and refinement details are shown in Tables 2, 3, and 4. Crystallographic data have been deposited with Cambridge Crystallographic Data Centre: Deposition numbers CCDC-1020229, CCDC-1020230, CCDC-1020231, CCDC-1020232, CCDC-1020233, CCDC-1020234, and CCDC-1020235 for compounds **1b**·H_2O, **6**, **7**·CH_2Cl_2, **8**·0.5$CHCl_3$, **9**·$CHCl_3$, **11**, and **12**, respectively. Copies of the data can be obtained free of charge via http://www.ccdc.cam.ac.uk/conts/retrieving.html (or from the Cambridge Crystallographic Data Centre, 12, Union Road, Cambridge, CB2 1EZ, U.K.; Fax: +44 1223 336033; e-mail: deposit@ccdc.cam.ac.uk).

This work was partially supported by Grant-in-Aid for Scientific Research (C) from Japan Society for the Promotion of Science (JSPS). We are grateful to Professor Soichiro Kyushin, Graduate School of Technology, Gunma University for his kind permission to use his single-crystal X-ray diffractometer.

Table 4. Crystal data and refinement details for **11** and **12**

	11	**12**
Empirical formula	$[C_{24}H_{26}ClPPdS_3]$	$[C_{24}H_{26}ClPPtS_3]$
Formula weight	583.45	672.14
Temperature/K	123(2)	123(2)
Crystal system	monoclinic	monoclinic
Space group	$P2_1$ (No. 4)	$P2_1/n$ (No. 14)
a/Å	9.6288(5)	8.7897(5)
b/Å	9.4346(5)	18.7062(11)
c/Å	13.6426(9)	15.5083(11)
α/deg	90	90
β/deg	93.5854(8)	95.8935(10)
γ/deg	90	90
V/Å^3	1236.92(12)	2536.4(3)
Z	2	4
D_{calc}/Mg m^{-3}	1.567	1.760
Absorp coeff/mm^{-1}	1.186	5.957
Crystal size/mm	0.30 × 0.20 × 0.10	0.30 × 0.20 × 0.10
θ range	2.63 to 27.50°	2.55 to 25.50°
No. of reflns meads	10439	13191
No. of indep reflns	5315	4688
R_{int}	0.0158	0.0233
Completeness	93.0%	99.1%
Data/Restraints/Parameters	5315/1/271	4688/0/299
Goodness–of–fit on F^2	1.055	1.367
Final R indices $[I > 2\sigma(I)]$[a)]	$R_1 = 0.0198$	$R_1 = 0.0296$
	$wR_2 = 0.1540$	$wR_2 = 0.0738$
	$wR_2 = 0.0483$	$wR_2 = 0.0578$
R indices (all data)[a)]	$R_1 = 0.0201$	$R_1 = 0.0302$
	$wR_2 = 0.1757$	$wR_2 = 0.0754$
	$wR_2 = 0.0486$	$wR_2 = 0.0579$
Absolute structure parameter	−0.004(17)	
Largest diff. peak and hole/e Å^{-3}	0.389 and −0.532	0.763 and −0.739

a) $R_1 = \Sigma||F_o| - |F_c||/\Sigma|F_o|$, $wR_2 = [(\Sigma w(F_o^2 - F_c^2)^2/\Sigma w(F_o^2)^2]^{1/2}$.

References

1 A recent review, see: L. Wang, W. He, Z. Yu, *Chem. Soc. Rev.* **2013**, *42*, 599.

2 R. Angelici, *Organometallics* **2001**, *20*, 1259.

3 J. Chen, R. Angelici, *Coord. Chem. Rev.* **2000**, *206–207*, 63.

4 C. Bianchini, A. Meli, *J. Chem. Soc., Dalton Trans.* **1996**, 801.

5 J. F. W. McOmie, *Protective Groups in Organic Chemistry*, London and New York, **1973**. doi:10.1007/978-1-4684-7218-9.

6 T. Yamamura, M. Tadokoro, K. Tanaka, R. Kuroda, *Bull. Chem. Soc. Jpn.* **1993**, *66*, 1984.

7 T. Yamamura, M. Tadokoro, R. Kuroda, *Chem. Lett.* **1989**, 1245.

8 S. Gruschinski, M. Handke, B. Kersting, *Z. Anorg. Allg. Chem.* **2012**, *638*, 1274.

9 L. Lindoy, S. E. Livingstone, T. N. Lockyer, *Nature* **1966**, *211*, 519.

10 Cleavage of C(sp^3)–S bond by platinum(0) complex has been reported: N. Nakata, N. Furukawa, T. Toda, A. Ishii, *Angew. Chem., Int. Ed.* **2010**, *49*, 5784.

11 A. S. Borovik, *Acc. Chem. Res.* **2005**, *38*, 54.

12 X. Hu, K. Meyer, *J. Organomet. Chem.* **2005**, *690*, 5474.

13 C. Pettinari, F. Marchetti, A. Drozdov, in *Comprehensive Coordination Chemistry II*, ed. by A. B. P. Lever, T. J. Meyer, Elsevier Pergamon, Oxford, **2004**, Vol. 1, pp. 211–251. doi:10.1016/B0-08-043748-6/01062-8.

14 G. Huttner, J. Strittmatter, S. Sandhöfner, in *Comprehensive Coordination Chemistry II*, ed. by A. B. P. Lever, T. J. Meyer, Elsevier Pergamon, Oxford, **2004**, Vol. 1, pp. 297–322. doi:10.1016/B0-08-043748-6/01082-3.

15 J.-C. Hierso, R. Amardeil, E. Bentabet, R. Broussier, B. Gautheron, P. Meunier, P. Kalck, *Coord. Chem. Rev.* **2003**, *236*, 143.

16 R. R. Schrock, *Acc. Chem. Res.* **1997**, *30*, 9.

17 N. Takeda, Y. Tanaka, F. Sakakibara, M. Unno, *Bull. Chem. Soc. Jpn.* **2010**, *83*, 157.

18 Group 10 metal complexes bearing analogous ligands, tris(methylthiophenyl)phosphine, have been reported: a) G. Dyer, D. W. Meek, *Inorg. Chem.* **1965**, *4*, 1398. b) G. Dyer, M. O. Workman, D. W. Meek, *Inorg. Chem.* **1967**, *6*, 1404. c) L. P. Haugen, R. Eisenberg, *Inorg. Chem.* **1969**, *8*, 1072. d) E. W. Abel, J. C. Dormer, D. Ellis, K. G. Orrell, V. Šik, M. B. Hursthouse, M. A. Mazid, *J. Chem. Soc., Dalton Trans.* **1992**, 1073.

19 S. B. Harkins, J. C. Peters, *J. Am. Chem. Soc.* **2004**, *126*, 2885.

20 W. Bauer, P. A. A. Klusener, S. Harder, J. A. Kanters, A. J. M. Duisenberg, L. Brandsma, P. v. R. Schleyer, *Organometallics* **1988**, *7*, 552.

21 A. G. Orpen, L. Brammer, F. H. Allen, O. Kennard, D. G. Watson, R. Taylor, *J. Chem. Soc., Dalton Trans.* **1989**, S1.

22 A. Bondi, *J. Phys. Chem.* **1964**, *68*, 441.

23 G. A. Barclay, R. S. Nyholm, R. V. Parish, *J. Chem. Soc.* **1961**, 4433.

24 The peak for CH_2=C of isobutene was also observed at 4.65 ppm.

25 For a recent paper, see: T. Okamura, K. Kunisue, Y. Omi, K. Onitsuka, *Dalton Trans.* **2013**, *42*, 7569.

26 C. G. Gutierrez, L. R. Summerhays, *J. Org. Chem.* **1984**, *49*, 5206.

27 D. H. R. Barton, D. Crich, A. Löbberding, S. Z. Zard, *J. Chem. Soc., Chem. Commun.* **1985**, 646.

28 I. Arai, T. Yamaguchi, Y. Hida, Process for the Preparation of Aromatic Sulfur Compounds. PCT int. Appl. 20000316, March 16, **2000**.

29 W. Armarego, C. Chai, *Purification of Laboratory Chemicals*, 6th ed., Butterworth-Heinemann, Oxford, **2009**.

30 G. M. Sheldrick, *SHELXS-97* and *SHELXL-97, Program for the Refinement of Crystal Structures*, University of Göttingen, Göttingen, Germany, **1997**.

31 A. Altomare, M. C. Burla, M. Camalli, G. L. Cascarano, C. Giacovazzo, A. Guagliardi, A. G. G. Moliterni, G. Polidori, R. Spagna, *J. Appl. Crystallogr.* **1999**, *32*, 115.